Study of the properties of atomic nuclei with the aid of muonic atoms

R. Engfer, H.-K Walter, and H. Schneuwly

Technical College, Zurich
Physics Institute of Freiburg University
Fiz. El. Chast. Atom. Yad., 5, 382-418 (April-June 1974)

Experimental investigations of muonic atoms are used to study the following problems in the physics of atomic nuclei: charge distribution, muonic isomer shift, polarizability of the nucleus by the muon, and the influence of the spatial distribution of the magnetization on the hyperfine splitting of the x-ray emission of the muon and on the nuclear gamma radiation (the Bohr–Weisskopf effect). The hyperfine electric quadrupole splitting of muonic x-ray emission and the possibility of an independent determination, with the aid of a precise model, of the quadrupole moment of the ground state of the nucleus are discussed. Comparison with other methods is used to examine the universality of the electron–nucleon and muon–nucleon interactions, to check on quantum electrodynamics, and to consider the "calibration" of the Mössbauer isomer shift and of the quadrupole splitting in pionic atoms.

INTRODUCTION

The Coulomb field of the nucleus of an ordinary atom in the bound state contains Z electrons. However, any other negatively-charged particles can also become a component part of the atom. Such an atom is called exotic, to distinguish it from an ordinary atom. If the particle is quasistable, i.e., its lifetime exceeds the duration of atomic processes, then it has time to execute a number of transitions over the orbits. These transitions are accompanied by x-ray emission. The characteristics of particles that can form exotic atoms are listed in Table 1, which contains also references to experiments in which such systems were observed.

The considerable interest in exotic atoms is due to their unique properties. The masses of negatively charged particles are at least 200 times larger than the electron mass. The Bohr orbits of such particles are therefore situated deep in the interior of the electron shell of the atom, so that the exotic atoms are hydrogen-like. The calculation of such systems reduces to a solution of the equations of the two-body problem, namely the Dirac equation for spin-1/2 particles and the Klein–Gordon equation for 0-spin particles. The wave functions of the higher-excited bound states overlap weakly the region where the charge of the atomic nucleus is distributed. The transitions between these states are used to study the properties of the negatively charged particles themselves, namely the mass (μ^-, π^-, K^-, $\bar{p}$), the magnetic moment (Σ^-), or the corrections for the vacuum polarization (μ^-). In the case of the low-lying levels, the overlap with the region of the nucleus is large, and the transitions are used to study nuclear properties.

In the sections that follow we discuss several experimental results on nuclear properties, as well as the progress made in the measurement techniques. The text of this review is based on four lectures delivered by Engfer in Dubna and Leningrad. The problem is dealt with in a large number of very good reviews,[30,39,51,61,93,99,100] and we confine ourselves to a discussion of new results and further trends in the development of research in this field. We pay principal attention to research carried out with the CERN muon channel during the last four years, with participation of representatives from the following four institutions:

The Hahn–Meitner Institute of Nuclear Research (U. Jahnke, K. H. Lindenberger, R. Mickelsen, G. Roschert);

The Institute of Technical Nuclear Physics of the Higher Technical School in Darmstadt (H. Backe, E. Kankeleit, R. Link, W. U. Schroder, K. Wien);

The Physics Institute of the Freiburg (Switzerland) University (T. Dubler, B. Robert-Tissot, L. Schellenberg, H. Schneuwly);

The Technical School and the Swiss Institute of Nuclear Physics in Zurich (R. Engfer, A. H. von Gunten, L. Flury, J. L. Vuillermier, S. Petitjean, H. K. Walter, A. Zender).

1. PRECISION MEASUREMENTS OF γ TRANSITION ENERGIES IN MUONIC ATOMS

Modern Ge(Li) detectors make it possible to measure the absolute values of the γ-quantum energies in μ atoms with a high degree of accuracy. Thus, the measurement error is about 15 eV at a quantum energy 100 keV, and about 0.5 keV at 6 MeV. In some investigations it has been possible to observe transitions from very high excited states (up to n = 16; see Fig. 2 of ref. 39). A typical γ-quantum spectrum, including a complicated combination of transitions, is shown in Fig. 1. The cascade transitions in the μ atom can be broken up into three groups, depending on the radii of the orbits between which they take place:

1) Transitions between the levels for which the principal quantum number takes on values $n \leq 3$. In this case the wave function of the muon strongly overlaps the region of the nuclear charge distribution, and the characteristics of such transitions are very sensitive to the concrete form of the distribution. This is why the transitions of the first group were intensively investigated in the past. We shall not discuss here this entire problem, but shall dwell only on certain new aspects connected with the determination of the radius of the nuclear charge distribution from data on transitions in muonic atoms.

2) Transitions between levels for which the overlap with the nucleus is small or practically nonexistent, but the corresponding orbits are below the electron orbits (in the case of heavy atoms these are orbits with $3 < n < 6$). The characteristics of such transitions depend only on the electromagnetic interaction of the muon, so that we can investigate different effects predicted by quantum electrodynamics.

3) Transitions between highly excited states ($n > 6$),

TABLE 1. Characteristics of Particles Capable of Forming Exotic Atoms. The Electron is Listed Only for Comparison; a_B is the Bohr Radius in Hydrogen. The Parentheses Contain the Measurement Errors

Particle	Spin	Mass, MeV	Lifetime, 10^{-10} sec	a_B, F	Experiments*
e^-	1/2	0.511006(2)		52917	—
μ^-	1/2	105.659(2)	2198.3(8)	256	—
π^-	0⁻	139.578(13)	260.4(7)	194	[8, 10]
K^-	0⁻	493.82(11)	123.5(4)	54.7	[10]
Σ^-	1/2+	1197.32(11)	1.64(6)	22.6	[10]
Ξ^-	1/2+	1321.7(7)	1.66(4)	20.5	None
Ω^-	3/2+	1672.4(6)	1.3(4)	16.2	None
$\bar{p}^-$	1/2+	938.256(5)		28.8	[11]

*Only basic papers are indicated; see the bibliographies in these papers.

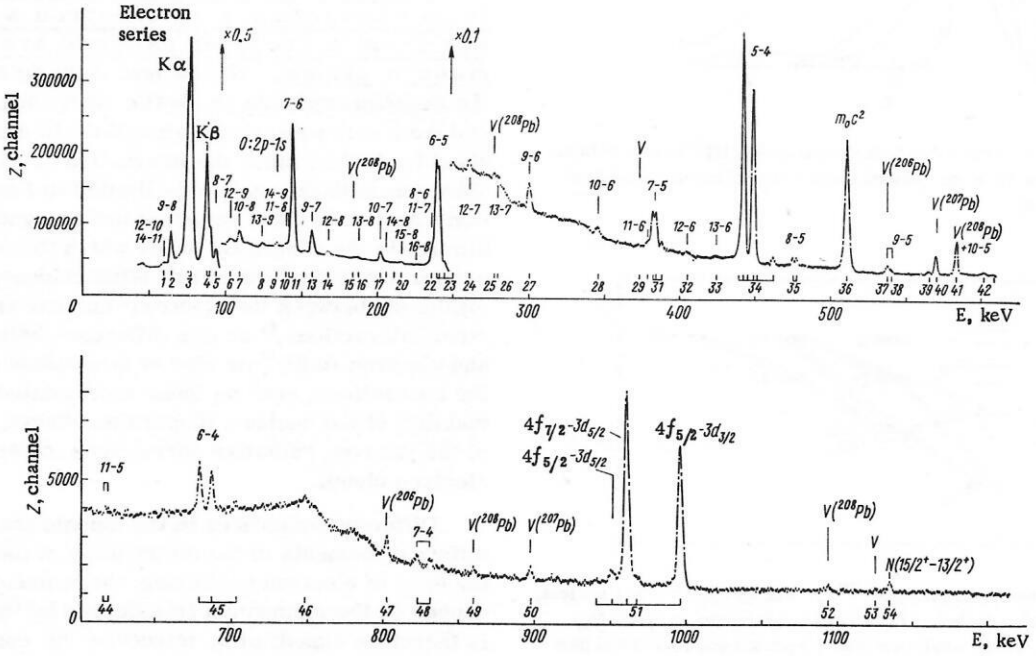

Fig. 1. Spectrum of prompt x-ray emission in the muonic ^{209}Bi atom (from the data of ref. 4). Each line can be set in correspondence either with a transition between definite states of the muonic ^{209}Bi atom with principal quantum numbers $n \to n'$, or a transition in the muonic oxygen atom that constitutes the background, or else an electronic K-series transition in the atoms Pb and Bi, as well as a delayed γ transition due to muon capture by the proton of the nucleus (designated by the letter V) and a prompt nuclear transition in the muonic ^{209}Bi atom (designated by the letter N). The following three prompt γ-quantum lines could not be identified in the spectrum: 39 (56.5 keV), 42 (601.7 keV), and 43.

whose principal quantum numbers differ by several units ($\Delta n > 1$) and whose orbits overlap with the electron orbits. The study of these transitions makes it possible to determine the distribution of the electron-cloud density in the atom.[51]

In the sections that follow we shall discuss certain new results pertaining to the first two groups of transitions. Only a few investigations are devoted to the transitions of the third group and deal with the influence of the electron cloud on the muon binding energy. The corresponding results are shown in Table 1 of ref. 39 and in Table 1 of ref. 5. The employed distributions of the electron density in the atoms have led to results that agree with the experimental data.[26,42,44,88] However, to distinguish between the details of the employed approximations it is necessary to increase the measurement accuracy by reducing the error to several electron volts. Such an accuracy will make it possible to observe also effects connected with the restructuring of the electron shell during the course of muon cascade transitions.

Nuclear charge distribution. The high sensitivity of the characteristics of a bound muon to the charge density distribution is illustrated in Fig. 2. For heavy atoms, the radii of the $2s_{1/2}$, $2s_{1/2}$, $2p_{1/2}$, and $2p_{3/2}$ orbits are of the same order of magnitude as the nuclear dimensions. The effects due to the finite nuclear dimensions can therefore no longer be regarded as small corrections to the results obtained for a point nucleus. The binding energies of the low-lying levels are compared in Fig. 3 for the case of a point and extended Tl nucleus. It follows from the presented data that it is the $1s_{1/2}$, $2s_{1/2}$, and the two 2p levels which are mainly sensitive to the character of the nuclear charge distribution. From the transitions between the indicated states one can determine at most three independent parameters. The wave functions of the different levels overlap differently with the region of the

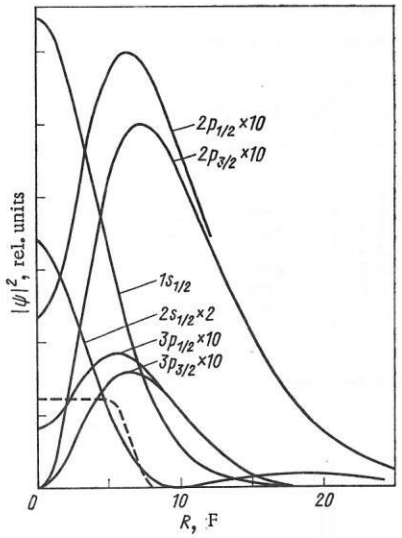

Fig. 2. Dependence of the muon density distribution $|\psi|^2$ on R in different states of the muonic Tl atom: dashed curve – region where the nuclear charge is distributed.

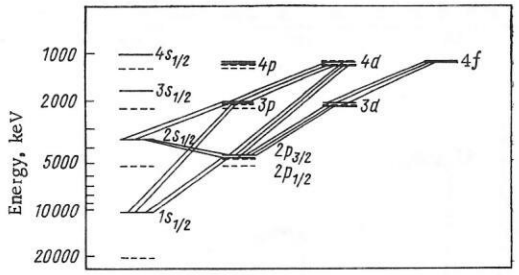

Fig. 3. Level scheme of muonic atom ^{205}Tl: dashed curve – point nucleus, solid curve – extended nucleus. Transitions in which the $3s_{1/2}$ and $4s_{1/2}$ states participate are very weak (less than 1% per stopped muon) and have not yet been observed.

nuclear charge distribution, so that each state determines an independent distribution parameter. A good illustration of this statement is Fig. 11 of ref. 5. The measured transition energies were analyzed in that reference within the framework of a two-parameter Fermi distribution of the density (with parameters c and t). In such an approach, however, it was impossible to account for the experimental data, so that it became necessary to introduce a third parameter[5] to take into account the nuclear polarization. Its value turned out to be 8 keV for the $1s_{1/2}$ level of the muonic atom of ^{203}Tl. Thus, allowance for the polarizability of the nucleus leads to a shift of the muon level in the atom. This correction was calculated in many papers.[27,40,41,74,75,82] The obtained values agree on the whole with the experimental data.[2,5,56,57] It must be borne in mind, however, that the experimental values themselves are the results of a mathematical reduction of primary data and depend strongly on the methods used in the reduction. Since the influence of the polarizability on the level shifts is not very well known, this limits at present the accuracy with which the nuclear charge distribution parameters are determined.

The fact that light nuclei have finite dimensions influences only the characteristics of the $1s_{1/2}$ level, and furthermore to a much lesser extent than in the case of heavy nuclei. In light muonic atoms we can therefore find only one charge-distribution parameter. In particular, for the muonic carbon atom the energy of the $2p_{1/2} \rightarrow 1s_{1/2}$ transition is 75.248 keV, and the effect due to the finite dimensions amounts to 394 eV. Taking into account the ± 15 eV measurement error we find that the nuclear radius is determined with an approximate accuracy of 4%. The shift depends little on the model representations used in the calculation, and the obtained value of the mean squared radius can be regarded as model-independent. The measured radii of several light nuclei, including the latest experimental data,[6,34] are listed in Table 2.

Comparative analysis of results obtained from experiments on electron scattering and from a study of cascade transitions in muonic atoms. The nuclear radii determined from the experimental data on elastic scattering of electrons and from data on cascade transitions in muonic atoms should coincide, since the interaction of the muons and electrons with the nucleus is limited to Coulomb attraction. Any observable deviation not connected with uncertainties in the conditions under which the concrete experiment was performed will offer evidence either of a difference between the electron–nuclear and muon–nuclear interactions,[13] or of a difference between the muon and electron radii,[78] or else of incomplete allowance for the corrections, such as those necessitated by the polarizability of the nucleus, dispersion effects, polarization of the vacuum, radiative corrections, or screening by the electron cloud.

Different transitions in the muonic atom determine different moments in the distribution of the nucleus. In the case of electron scattering, the moments turn out to depend on the momentum transferred by the electron. It is therefore expedient to introduce the concept of the equivalent momentum transfer q, at which the model dependence of the results of data extracted from electron scattering and from cascade transitions in the atom is the same. According to ref. 36, this momentum is given by

$$q^2 = 6Z \Big/ \left[\frac{5}{3}\langle r^2\rangle^{1/2} a_B\right], \qquad (1)$$

where a_B = 256 F, corresponding to scattering of electrons with approximate energy 50 MeV. The data obtained at higher incident-electron energies, say 500 MeV, are much more sensitive to the details of the charge distribution. In this case, however, we obtain information not on the mean squared radius $\langle r^2\rangle$, but on charge-distribution moments higher than the second. The discrepancies between the electronic and atomic data at such energies can therefore be attributed to the model dependence, whereas at equivalent momentum transfers the model dependence hardly comes into play.

The radii of nuclei in the region of iron were compared in ref. 78 with allowance for the equivalent momentum transfer. The agreement obtained between the muonic-atom data and electron-scattering data was very good when the results of the electron scattering were normalized to the ^{12}C radius determined by the Amsterdam

TABLE 2. Mean Squared Radii of the Nuclei ^{12}C, ^{14}N, and ^{16}O, Obtained from Muonic Atoms and from Experimental Data on Electron Scattering. All the Quantities are in Fermi Units

^{12}C	^{14}N	^{16}O	Experiments	Reference
2.40±0.02	—	2.65±0.04	(e, e) 183 MeV	[28]
2.42±0.04	—	—	(e, e) 50 MeV	[37]
—	2.64	—	(e, e) 400 MeV	[29]
2.460±0.025	—	2.730±0.025	(e, e) 375; 750 MeV	[83]
2.445±0.015	—	—	(e, e) 20—80 MeV	[55]
2.453±0.008	—	—	Shell model	[55]
2.395±0.028	2.492±0.033	2.666±0.033	(e, e) 30—60 MeV Shell model	[16]
2.454±0.03	2.56±0.03	2.70±0.03	(e, e) 31—60 MeV	[81]
2.40±0.56	2.67±0.26	2.61±0.14	Muonic atoms	[7]
2.49±0.05	2.55±0.03	2.70±0.02	Muonic atoms	[6]

group.[55] If the normalization is against the result of the Darmstadt group, obtained with a gas target,[16] the discrepancy is of the order of two standard deviations. The latest data on transitions in the muonic ^{12}C atom show that the mean squared radius obtained in such measurements agrees with the data of the Amsterdam group on elastic scattering and with the old Darmstadt results obtained by using carbon foils.[37] This means that the Darmstadt measurements with a gas target are subject to a systematic error. Recent calculations with the experimental data of ref. 81 has indeed led to a larger value of $\langle r^2 \rangle$ and to better agreement with the results of the Amsterdam group. The mean squared radii of ^{12}C, obtained by different groups, are given in Table 2.

Starting with the agreement of the measured values of $\langle r^2 \rangle$, we can draw the conclusion that no difference was observed between the muon–nucleon and electron–nucleon interactions. This contradicts the theoretical estimates in which a neutral pseudoscalar meson was introduced as an intermediate particle.

From the data of Table 2 we can establish[6,34] an upper bound on the difference between the muon and electron radii. This limit is $\langle r_\mu^2 \rangle - \langle r_C^2 \rangle \leq 0.17$ F^2 and agrees with the value ≤ 0.014 F^2 obtained from a comparison of the results of ep and μp scattering at high energies, and with the value ≤ 0.004 F^2, obtained by measuring the (g − 2) factor.

Use of muonic atoms to check on quantum electrodynamics. The most important correction to the muon binding energy in the atom is due to the polarization of the vacuum (or renormalization of the charge). It is known that in an ordinary electronic atom this correction is small in comparison with the Lamb shift (mass renormalization). In a muonic atom, owing to the difference between the muon and electron masses, the situation is reversed. The Lamb shift leads to a decrease of the binding energy in an ordinary atom, and the small increase due to allowance for the vacuum polarization can be neglected. In the muonic atom, on the contrary, the binding energy increases, since the main correction is connected with the polarization of the vacuum. In the light muonic atoms (μH) and (μHe), for which the effect of the finite nuclear dimensions is small, the $2s_{1/2}$ state is more strongly bound than $2p_{1/2}$ and is metastable. This does not occur in heavy muonic atoms, where the effect of the finite dimensions is much stronger than the radiative corrections.

The Lamb shift has been measured in electronic atoms, in experiments on electron scattering, and in the determination of the (g − 2) factor.[64] The effect due to vacuum polarization can be measured in muonic atoms (such measurements were performed in refs. 15, 18, 43, and 46, where earlier investigations are cited). To determine the transitions that are best used for the measurement of definite characteristics, let us turn to Tables 3 and 4. These tables list the shifts, due to different effects, of certain levels of the muonic atoms of H, He, and ^{203}Tl, respectively. It follows from the data presented that the vacuum polarization effect is best determined either on the basis of the metastable $2s_{1/2}$ level of muonic H or He, or in medium and heavy atoms in transitions with principal quantum numbers $4 \rightarrow 3$ and $5 \rightarrow 4$. Measurements of the $2s_{1/2} \rightarrow 2p_{1/2}$ transition energies in muonic H are now underway at CERN.[102] It should be noted, however, that there is still no experimental procedure for obtaining the absolute values of the γ-quantum energies in the region from 1 to 3 keV with an accuracy of several thousandths of an eV. This is why the $2p \rightarrow 1s$ transition in muonic H and He cannot yield the required information. In ref. 33 the authors measured $4 \rightarrow 3$ and $5 \rightarrow 4$ transitions for certain nuclei in the range from Z = 47 to 82. The experimental data reveal an appreciable discrepancy between theory and experiment, which depends furthermore on Z. This discrepancy is due in part to the subsequently observed error in the actual calculation of the radiative corrections, which had no bearing on the theory itself.[33] Errors were incurred in the determination of not only the values but also in the sign of the term of order $\alpha(\alpha Z)^3$ in the expression used to calculate the effects connected with vacuum polarization.[15,18] New calculations made it possible to decrease the discrepancy somewhat. This situation has made it necessary to repeat the measurements. This need was also brought about by the fact that the old experimental data[8,12] contradicted the later measurements.[33] The measurements for certain nuclei were repeated[90] with a new calibration system, which will be described later on. The results were in very good agreement with the data of ref. 33. A summary of these experimental data is given in Table 4.

Thus, the following situation has developed by now: In heavy muonic atoms there are discrepancies between

TABLE 3. Corrections to the $2s_{1/2} - 2p_{1/2}$ Energy Difference in Muonic Hydrogen (μH) and Muonic Helium (μHe) (refs. 20, 46)

Corrections to energy difference	μH, 10^{-3} eV	μHe, 10^{-3} eV
$2p_{1/2}-2p_{3/2}$, fine structure	8.416	145.7
Polarization of vacuum:		
of order α	−205.0	−1665.9
of order α^2	−1.508	−11.5
Lamb shift	+0.660	+14.3
Delay	+1.387	—
Finite nuclear dimensions*	+3.474±0.081	+293.7±7.0
$E(2s_{1/2})-E(2p_{1/2})$	−200.988±0.081	−1369.4±7.0
$E(2s_{1/2})-E(2p_{3/2})$	−209.404±0.081	−1515.1±7.0

*The rms radius $\langle r^2\rangle^{1/2}$(H) = 0.80 ± 0.02 F, used in the calculation, was taken from ref. 96. We present also later results obtained in experiments on electron scattering at a small momentum transfer ($\leq 0.4\,F^{-2}$), 0.82 ± 0.07 F (ref. 54), 0.85 ± 0.02 F (ref. 87); $\langle r^2\rangle^{1/2}$(He) = 1.67 ± 0.03 F.

TABLE 4. Theoretical Calculations of the Transition Energies in the Muonic ^{203}Tl Atom, from the Data of refs. 5 and 90

Transition	Total transition energy, eV	Vacuum polarization, eV			Other electrodynamic corrections*	Polarizability of the nucleus, eV	Electron screening, eV	Finite dimensions of nucleus, eV
		α	α^2	higher orders				
$2p_{3/2}-1s_{1/2}$	5 906 630	37 520	930	**	−3570	4900	−4	−9 839 700
$2p_{1/2}-1s_{1/2}$	5 725 890	34 750	870	**	−2800	5000	−4	−9 499 000
$3d_{5/2}-2p_{3/2}$	2 448 060	19 380	−50	**	−1000	1800	−13	−219 900
$3d_{3/2}-2p_{1/2}$	2 587 970	21 330	−60	**	−320	1870	−13	−558 400
$5g_{9/2}-4f_{7/2}$	420 777	2 038	32	−49	−4	5	−80	−3
$5g_{7/2}-4j_{5/2}$	426 881	2 117	30	−47	11	6	−78	−9

*Including the correction for the Lamb shift, for the anomalous magnetic moment, for the relativistic reduced mass, and for the muonic polarization of vacuum.

**These corrections are smaller than the measurement errors of the transitions in question.

theory and experiment, on the order of two standard deviations, which cannot be eliminated even if all the known corrections are taken into account. It is necesary, however, to bear in mind the uncertainties in the calculations of the higher terms of the radiative corrections. The errors that arise in the calculation of the screening by the electron cloud are smaller than the experimentally observed[44] discrepancies. They can be attributed to screening only by making very unlikely assumptions concerning the character of the electron-density distribution. A difference may also take place in the μN and eN interactions, as indicated in refs. 13 and 14. However, since the nuclear radii obtained from data on muonic atoms and from experiments on electron scattering are equal, it becomes necessary to analyze in greater detail assumptions of this type also in the calculation of radiative corrections. If the experimental energy of the $2s_{1/2} \rightarrow 2p_{1/2}$ transition in muonic helium[102] turns out subsequently to agree with the theoretical value, then this fact will not contradict the existing discrepancies in the case of heavy muonic atoms (Fig. 4). The point is that the error that arises in the calculation in terms of higher order in αZ is negligibly small for muonic atoms with small Z.

2. MAGNETIC HYPERFINE INTERACTION IN MUONIC ATOMS

Theoretical analysis. The muon is a lepton, so that the magnetic hyperfine interaction of a muon with an atomic nucleus in a muonic atom is perfectly analogous to the hyperfine interaction in an ordinary electronic atom. The shift of the hyperfine component of the level is determined by the Fermi−Segree equation

$$\Delta W_m = A_I(I,\ nlj)\,\frac{[F(F+1)-I(I+1)-j(j+1)]}{2Ij}. \qquad (2)$$

If we confine ourselves to the muon $1s_{1/2}$ level, then j = 1/2 and F = I ± 1/2. In this case we have doublet splitting amounting to

$$\Delta E_m = A_I(I;\ 1;\ 0;\ 1/2)\,\frac{2I+1}{I}. \qquad (3)$$

For a point nucleus, the hyperfine splitting constant A_I(I, nlj) is proportional to $\mu_I H_\mu$. Unlike the electron in an ordinary atom, a muon on the $1s_{1/2}$ orbit of a heavy muonic atom produces a very strong magnetic field, with intensity on the order of $H = 10^{13}$ G. We can therefore expect the magnetic splitting to be of the order of 1 keV/u. The radius of the first Bohr orbit of the muon is comparable with the dimensions of the nucleus. The magnetic field produced is therefore inhomogeneous, and the magnetic splitting depends strongly on the nature of the distribution of the magnetization in the nucleus.

In ordinary atoms, effects connected with the finite

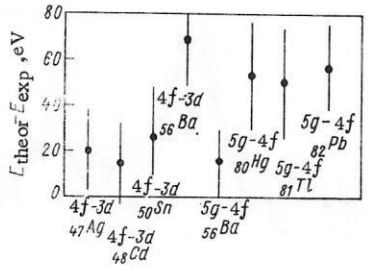

Fig. 4. Deviation of the theoretical values of the energies of the $4f \rightarrow 3d$ and $5g \rightarrow 4f$ transitions from the experimental values[8,12,33,90] in certain muonic atoms.

size of the nucleus are small.[19] Moreover, it is impossible to determine the value of this effect for each isotope, since the absolute value of the density distribution of the electrons in an ordinary atom cannot be measured. Optical spectroscopy methods[35,84] can determine only the relative magnitude of the effect in different isotopes. Let us consider, for two isotopes a and b, the expression

$$\Delta_{ab} = (A_a^{\exp}/A_b^{\exp})(g_b^{\exp}/g_a^{\exp}) - 1 \approx \varepsilon_a - \varepsilon_b, \qquad (4)$$

where

$$A^{\exp} = A^{\text{point}}(1+\varepsilon).$$

The quantity Δ_{ab} determines the difference between the effects due to the finite nuclear size in the two isotopes. In the case of a muonic atom, the muon distribution density is calculated with a high degree of accuracy by solving the Dirac equation. We can therefore calculate the effect for each isotope with allowance for the character of the distribution of the nuclear magnetism. Such calculations were performed first in ref. 65 (see also refs. 38 and 59). The expression for A_I is

$$A_I = -\frac{4}{3} e\mu_0\mu_I \left\langle \Phi_I \Big/ \int_0^R f(r)\, g(r)\, (r/R)^3\, dr + \int_R^\infty f(r)\, g(r)\, dr/\Phi_I \right\rangle. \qquad (5)$$

To calculate this quantity it is necessary to know the wave function Φ_I, i.e., it is necessary to use a definite model.

Magnetic hyperfine splitting and x-ray emission energies in muonic atoms. The magnetic hyperfine splitting of the $2p_{1/2} - 1s_{1/2}$ line in heavy muonic atoms can be determined only from the broadening, inasmuch as at high energies (3.4 and 6 MeV in the muonic atoms of In and Bi, respectively) the resolution of even the best detectors is only 3.5 and 5 keV, respectively. This analysis, however, is very complicated and is not at all unambiguous, since it is necessary to determine the shape of the experimental curve on the basis of the calibration curve, which is a priori not identical with the experimental curve. In addition, it is necessary to take into account the Lorentz broadening, the magnitude of which is of the order of half a keV. A typical situation is shown in Fig. 8 of ref. 77, with ^{209}Bi as an example. The magnetic hyperfine splitting is also influenced by effects due to nuclear polarizability (see below); the corresponding correction can reach 25%, as is the case in the ^{209}Bi muonic atom.[77]

Ge(Li) detectors have the best absolute resolution at low radiation energies. However, the magnetic hyperfine splitting of lines corresponding to transitions between high-lying states at low radiation energies is usually too small to be resolved. An exception is the $2s_{1/2} \rightarrow 2p_{1/2}$ transition. In addition, it has one more advantage: The levels $2s_{1/2}$ and $2p_{1/2}$ have different dependences on the character of the magnetization distribution in the nucleus than the level $1s_{1/2}$. It therefore becomes possible to determine different components of the magnetization distribution. In the case of a point nucleus, the $2s_{1/2}$ and $2p_{1/2}$ levels are degenerate. Allowance for the finite dimensions of the nucleus shifts the $2s_{1/2}$ level by a larger amount than the $2p_{1/2}$ level (for example, in the ^{115}In muonic atom this difference is 260 keV), so that transitions between these states can be observed. The probability of populating the $2s_{1/2}$ level in cascade transitions, however, is very small (~1.5%), and to accumulate the required statistics, rather long accelerator operating time is necessary. The level scheme of the ^{115}In muonic atom is shown in Fig. 5, and the corresponding experimental spectrum is given in ref. 69. Analogous data on the Nb muonic atom can be found in ref. 76.

The measured values of the hyperfine splitting of the $2p_{1/2}$ level must be corrected for the "pseudomagnetic splitting".[71,76] The point is that, in first-order perturbation theory, the quadrupole hyperfine interaction leads to a splitting of the $2p_{3/2}$ level and does not influence the $2p_{1/2}$ level. In second order, however, these levels become intermixed. We shall demonstrate this with the ^{115}In muonic atom as an example. The quadrupole interaction in the hyperfine-structure states with spins F = 4 and 5 mixes the $2p_{1/2}$ and $2p_{3/2}$ components. The result, besides a small shift, is a pseudomagnetic splitting amounting to approximately 180 eV.

Magnetic hyperfine splitting of nuclear radiation in muonic atoms. The nucleus of many heavy muonic atoms becomes excited in the course of the cascade transitions of the muon. This is due to a random coincidence of the radiation energy and of the nuclear-level energy. The phenomenon itself will be discussed in detail later on. We note here, however, one

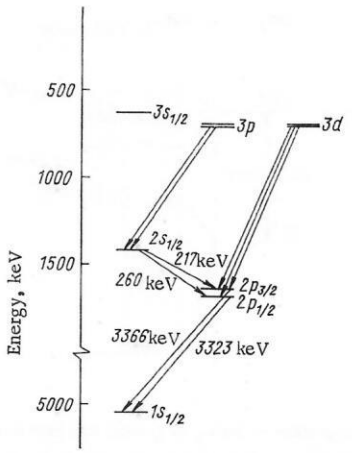

Fig. 5. Scheme of $2p \rightarrow 1s$ and $2s \rightarrow 2p$ transitions in the ^{115}In muonic atom.

important detail: A γ quantum is emitted from the excited state of the nucleus in the presence of a muon in the $1s_{1/2}$ orbit of the atom. The latter produces a magnetic field, whose intensity is of the order of 10^{13} G. As a result, both the ground and the excited states of the nucleus become split into doublets.[101] By way of example, Fig. 6 considers the case of the ^{205}Tl muonic atom. The electromagnetic M1 transition between the states of the doublet proceeds rapidly. Consequently only the splitting of the ground state, which is identical to the $1s_{1/2}$-level splitting observed in the $2p \rightarrow 1s$ transition, affects the γ-radiation spectra. Since the energy of the nuclear γ radiation is much smaller than the energy of the $2p \rightarrow 1s$ transition, the magnetic hyperfine splitting can be easily resolved with the aid of Ge(Li) detectors. The hyperfine-splitting constant can therefore be determined with much greater accuracy. The spectrum of the nuclear transitions in the ^{203}Tl muonic atom in the energy interval 275-282 keV is shown in Fig. 7. The corresponding data for the ^{205}Tl muonic atom can be found in Fig. 3 of ref. 5.

Cascade transitions of a muon excite, with high probability, rotational 2^+ states of deformed nuclei. Owing to the presence of the muon, the excited 2^+ state splits into two. The rate of the electromagnetic transition between the states of the doublet is high, so that the splitting can be observed only in those cases when the nuclear transitions are also rapid. By way of example, Fig. 8 shows the case of the ^{190}Os muonic atom. The half-life of the 2^+ level in the ^{190}Os nucleus is 350 psec. The competing process is a transition between the doublet states and lasts 30 psec. Therefore the intensity of the γ transition from the upper state F = 5/2 of the hyperfine doublet is only 8%. In the total spectrum, this transition appears in the form of a slight distortion, on the high-energy side, of the strong line due to the transition from the lower state of the doublet, with spin F = 3/2. The corresponding experimental spectrum in the ^{190}Os muonic atom is shown in Fig. 9.

Comparison of experimental data on the hyperfine splitting in muonic atoms with theoretical predictions. The experimental and theoretical values of the magnetic hyperfine splitting are

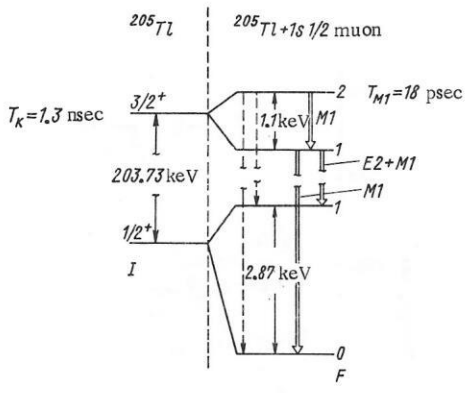

Fig. 6. Magnetic hyperfine splitting of ground and first excited states in the ^{205}Tl muonic atom (right). The same levels, but in the absence of the muon, are shown on the left. The splitting was calculated within the framework of the shell model with allowance for configuration mixing.[38]

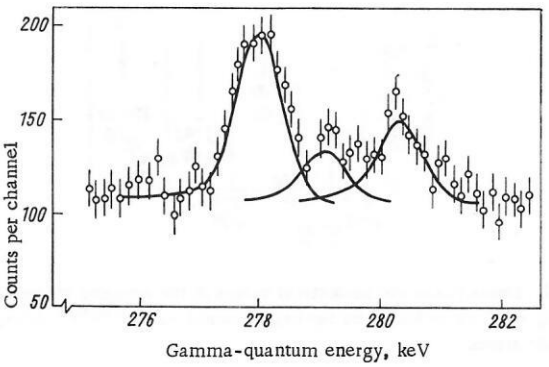

Fig. 7. Spectrum of prompt γ quanta in ^{203}Tl muonic atom (enriched target) in the region of nuclear $3/2^+ \rightarrow 1/2^+$ γ transition (energy $\sim$ 279 keV); solid curve – result of reduction of the experimental spectra. The two outer maxima are the result of the hyperfine splitting of the nuclear level in the muon field. The small central maximum is the same γ transition due to inelastic scattering of the delayed neutrons from the μ capture.

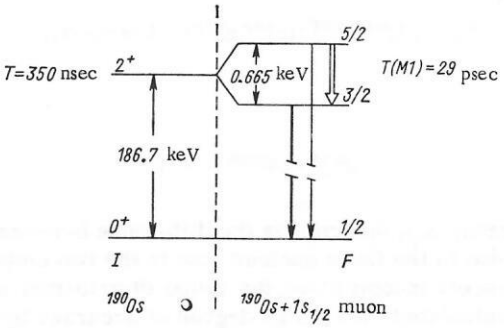

Fig. 8. Scheme of nuclear $2^+ \rightarrow 0^+$ γ transition in ^{190}Os muonic atom, in accordance with the data of ref. 70.

shown for a large number of atoms in Table 5. The experimental values[38,59] are much smaller than those calculated assuming a point distribution of the magnetic moment. Thus, in the case of the ^{115}In muonic atom, the hyperfine-splitting constants are,[1)] in this approximation, $A_1(1s_{1/2}) = 2.51$, $A_1(2p_{1/2}) = 0.628$, and $A_1(2s_{1/2}) = 0.425$ keV. As follows from Table 5, the experimental values are smaller by 35, 25, and 45%, respectively, than the theoretical ones. This indicates that the different muonic levels depend quite strongly, and in different manners, on the character of the magnetic-moment distribution.

The models describing the magnetization distribution in the nucleus should also account for the value of the magnetic moment. In odd nuclei, the magnetic moment is due to the magnetic moment of the unpaired particle, and the contribution of the core is usually small. Consequently, the properties of the unpaired nucleon can be assessed in principle from the magnetic splitting in the muonic atom. The results of calculations performed in different models agree with the experimental data. The difference between the results obtained in different models (model with configuration mixing, model with pairing, model with pairing and quadrupole–quadrupole interaction[59]) is too small in comparison with the measurement error, and it is therefore impossible to choose

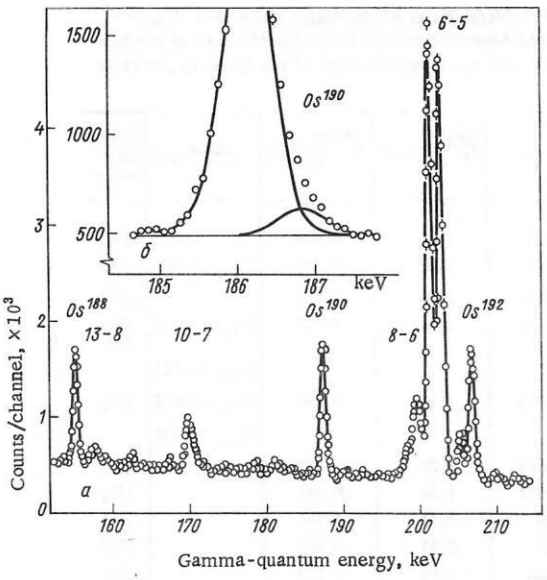

Fig. 9. Spectrum of prompt γ quanta in Os muonic atom[50] (natural isotope mixture). The x-ray transitions in the muonic atom are labeled with the principal quantum numbers of the $n \to n'$ levels. The γ line of the nuclear $2^+ \to 0^+$ transition is shown for each isotope (a). Insert: 187-keV nuclear $2^+ \to 0^+$ transition in ^{190}Os muonic atom and results of reduction of the spectrum with separation of the hyperfine-structure components (b). The half-life of the 2^+ level in ^{188}Os is large (710 nsec) so that the F = 5/2 component of the hyperfine structure is very weak in comparison with the principal component F = 3/2 (3.4%) and is not observed in the experiment.[71]

between them. The measurement error was small only in the case of the ^{203,205}Tl muonic atoms, for which it was possible to resolve fully the hyperfine structure of the nuclear γ lines. However, it is precisely for this case that all the calculations[5,38,59] lead to too large a splitting. For the electronic $1p_{1/2}$ level, the experimental value $\Delta_{ab}(^{203-205}\text{Tl}) = +(0.01050 \pm 0.00015)\%$ contradicts the theoretical[84] $\Delta_{ab} = (-0.041 \pm 0.017)\%$. This discrepancy has been eliminated in part in recent calculations, in which the results of the latest measurements of the isotopic shift were used. Nonetheless, further calculations of the hyperfine splitting in the optical and muonic-atom spectra are necessary.

Connected with the Tl muonic atom is another interesting problem pertaining to the excited $3/2^+$ level: If the spin part of the magnetic moment of the valence nucleon is cancelled out by the orbital part, then the total magnetic moment is very small. This effect is known in the literature as the Bohr–Weisskopf effect. For the $d_{3/2}$ proton, the magnetic moment is

$$\mu(3/2^+) = \frac{9}{5} g_p^l - \frac{3}{10} g_p^s = 0.124, \qquad (6)$$

where

$$g_p^l = 1 \text{ and } g_p^s = 5.584526.$$

This situation is typical, in particular, of the excited $3/2^+$ states of the nuclei ^{203,205}Tl, ^{197}Au, and ^{191,193}Ir. In the ^{205}Tl nucleus, without allowance for the spatial distribution of the magnetization, the splitting should be equal to $\Delta E^{\text{point}} = 0.24$ keV, and the value corresponding to an extended nucleus[38] is $\Delta E^{\text{ext}} = 1.11$ keV. In the case of level splitting in the muonic atom, there is no mutual cancellation, and to the contrary, the splitting should be four times larger than the value expected for a point nucleus. The Bohr–Weisskopf effect discussed above in muonic atoms has not been observed to this day. The state $3/2^+$, particularly in ^{203,205}Tl, can also be described on the basis of the weak-coupling model:[79] The proton in the $3s_{1/2}$ state is coupled with the excited core in the 2^+ state. According to this model, the magnetic splitting should be small. Therefore, an experiment in which it is possible to resolve the magnetic hyperfine splitting of the ground and excited states in a nuclear γ transition in the Tl muonic atom is capable of distinguishing between the two nuclear models.

The distribution of the magnetic moment in the excited 2^+ state of a deformed nucleus is due to collective motion of the charge. In the rigid-rotator model, in which the nucleus rotates as a rigid body about an axis perpendicular to the deformation axis, the magnetization distribution density is given by

$$M(R) \sim \int_R^\infty r\rho_c(r)\,dr, \qquad (7)$$

where $\rho_c(r)$ is the charge distribution density (see also ref. 101). For the 2^+ state of Os, it follows from this model that $A_I(^{190}\text{Os}) = 0.275$ and[70] $A_I(^{192}\text{Os}) = 0.331$ keV. This is in good agreement with the experimental values (see Table 5).

In the case of the ^{200}Hg nucleus, the agreement is better [$A_I(^{200}\text{Hg}) = 0.284$ keV] if $\rho_c(r)$ is replaced by the density $\rho_2(r)$, which takes into account only the rotation of the surface quadrupole charge.[71] The determination of this quantity can be found, in particular, in ref. 98. Calculations based on a microscopic description of the magnetization distribution in the 2^+ state of a deformed nucleus were performed in ref. 73. The distribution has two maxima corresponding to two different radii. The total magnetic moment turned out to be concentrated in the smaller radius, and the resultant magnetic splitting was larger in magnitude than that predicted by the model of a simple rigid rotator. The result obtained for the Os muonic atom was $A_I(^{190}\text{Os}) = 0.320$ and $A_I(^{192}\text{Os}) = 0.344$ keV, in good agreement with the experimental data. Moreover, the microscopic approach employed has made it possible to describe in addition both the magnetic moment[2)] and the isomer shift (see below).

3. NUCLEAR γ TRANSITIONS IN MUONIC ATOMS

Nuclear excitations in muonic atoms. The excitation of the levels of a deformed nucleus in the course of muon cascade transitions were investigated in refs. 53 and 95. The scheme of the processes is shown in Fig. 10. The parity and the total angular momentum of the states

$$\Psi_A = |2p_{3/2},\ 0^+,\ F = 3/2\rangle \text{ and } \Psi_B = |2p_{1/2},\ 2^+,\ F = 3/2\rangle$$

are the same (in this case, F = 3/2), and these two states

TABLE 5. Constant A_1 of the Hyperfine Splitting for Different Levels ($1s_{1/2}$, $2s_{1/2}$, $2p_{1/2}$, $2p_{3/2}$, $3d_{3/2}$, and $3d_{5/2}$) of Muonic Atoms. The Theoretical Values of This Quantity, Calculated Assuming a Point Magnetic Moment of the Nucleus, Are Shown for Comparison. The Calculation Was Carried Out with the Wave Function of the Muon in the Field of an Extended Nucleus

Isotope	$A_1^{exp}(1s_{1/2})$, keV	$A_1^{exp}(2p_{1/2})$, keV	A_1^{exp}, keV	μ_N	$A_1^{exp}(1s_{1/2})$, keV	$A_1^{theor}(2p_{1/2})$, keV	A_1^{theor}, keV	Reference
^{93}Nb(9/2+)	1.61±0.11	0.36±0.08		6.167	2.32	0.426		[25]
^{93}Nb(9/2+)	1.560±0.048	0.374±0.020[s]	$2s_{1/2}$: 0.227±0.023	6.167	2.32	0.426	$2s_{1/2}$: 0.356	[76]
^{115}In(9/2+)	1.65±0.07	0.55±0.13		5.5351	2.51	0.628		[66]
^{115}In(9/2+)	1.61±0.03	0.446±0.060[s]	$2s_{1/2}$: 0.236±0.060	5.5351	2.51	0.628	$2s_{1/2}$: 0.425	[69, 71]
			$2p_{3/2}$: 0.16±0.06				$2p_{3/2}$: 0.221	
^{127}I(5/2+)	0.89±0.09	0.294±0.089	$3d_{3/2}$: 0.045±0.005	2.8091	1.44	0.405	$3d_{3/2}$: 0.046	[67]
			$3d_{5/2}$: 0.030±0.005				$3d_{5/2}$: 0.032	
^{133}Cs(7/2+)	1.11±0.18	0.50±0.20		2.5789	1.34	0.405		[66]
^{139}La(7/2+)	1.35±0.08	0.48±0.08		2.7781	1.50	0.481		[25]
^{141}Pr(5/2+)	1.53±0.15	0.62±0.20		4.28	2.41	0.881		[66]
^{141}Pr(5/2+)	1.52±0.06			4.28	2.41	0.881		[58]
^{151}Eu(5/2+)	0.80±0.27			3.465	2.04	0.772		[21]
^{190}Os(2+)[m]	0.266±0.032[i]			0.662 [17]	0.447	—		[70]
^{192}Os(2+)[m]	0.320±0.032[i]			0.797 [62]	0.538	—		[70]
^{199}Hg(1/2−)	0.117±0.029[i]			0.502702	0.371	0.089		[71]
^{200}Hg(2+)[m]	$0.262\pm^{0.042}_{0.030}$[i]			0.43	0.318	0.076		[71]
^{203}Tl(1/2+)	0.642±0.040[i]			1.61169	1.201	0.639		[5]
^{205}Tl(1/2+)	0.575±0.008[i]			1.62754	1.213	0.644		[5]
			$2p_{3/2}$: 0.30±0.03				$2p_{3/2}$: 0.356	
^{205}Tl(1/2+)	0.61±0.03	0.53±0.06	$3d_{3/2}$: 0.091±0.010	1.62754	1.213	0.644	$3d_{3/2}$: 0.099	[25]
			$3d_{5/2}$: 0.054±0.006				$3d_{5/2}$: 0.065	
^{209}Bi(9/2−)	2.5±0.5	1.2±0.5		4.0802	3.07	1.702		[77]
^{209}Bi(9/2−)	2.1±0.2	1.1±0.1		4.0802	3.07	1.702		[22]
			$2p_{3/2}$: 0.69±0.08				$2p_{3/2}$: 0.944	
^{209}Bi(9/2−)	2.16±0.15	1.50±0.20	$3d_{3/2}$: 0.27±0.03	4.0802	3.07	1.702	$3d_{3/2}$: 0.269	[68]
			$3d_{5/2}$: 0.09±0.01				$3d_{5/2}$: 0.176	

[i] Obtained from hyperfine splitting of nuclear γ line in the presence of a muon in the $1s_{1/2}$ orbit.
[m] Splitting of first excited state of the nucleus.
[s] Corrected for the pseudomagnetic splitting due to the quadrupole mixing of the $2p_{3/2}$ and $2p_{1/2}$ states.

are quite close to each other in energy. In this case the mixing of the states A and B is determined by an interaction whose scale coincides with the distance $E_A - E_B$ between the levels. In deformed nuclei such a perturbation is an electric quadrupole interaction, the value of which amounts to 100–200 keV, and consequently always satisfies the resonance condition[49]

$$\left|\frac{E_A - E_B}{M}\right| \leqslant 1, \qquad (8)$$

where M $\langle \Psi_A | H | \Psi_B \rangle$ is the interaction matrix element.

However, quadrupole interaction between 2p levels of the fine structure is not the only one capable of exciting the nucleus. An interaction of different multipolarity can also cause excitation provided the condition for the onset of resonance is satisfied, and the spins and parities of the states of the system coincide. The types of resonance observed or predicted by now are E0 (ref. 48), E1 (ref. 85), E3 (refs. 4, 5, 23, 50), and M1 (refs. 1, 67).

Isomer shift in muonic atoms. A muon undergoing a cascade transition, say from the $3d_{5/2}$ level, populates with sufficiently high probability the states in which the nucleus is excited. The lifetime of the nuclear excitation is of the order of 10^{-9} sec. It is large in com-

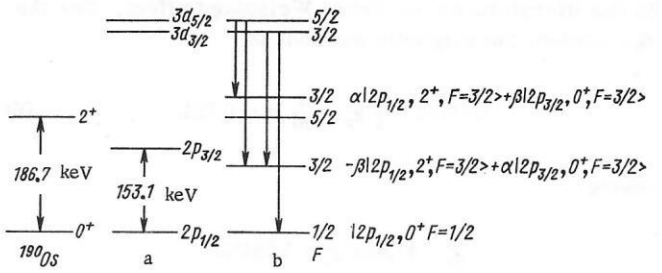

Fig. 10. Mixing of the $2p_{1/2}$ and $2p_{3/2}$ muonic states and 2^+ and 0^+ nuclear states, due to the dynamic electric quadrupole interaction in ^{190}Os. Only strong transitions are indicated: a) without allowance for nuclear-state mixing; b) with allowance for the mixing.

parison with the time within which the E1 transition takes place between the states $2p \rightarrow 1s$ (on the order of 10^{-14} sec). The muon therefore reaches the $1s_{1/2}$ ground state, whereas the nucleus remains excited. The muon lifetime in the $1s_{1/2}$ state is determined by the rate of its capture by the protons of the nucleus, and amounts to about 100 nsec, which is much longer than the lifetime of the excited state of the nucleus. As a result, the nuclear γ quanta are emitted in the presence of a muon in the $1s_{1/2}$ orbit.

In addition to the magnetic hyperfine splitting, the presence of the muon leads also to a shift of the excited-state energy, due to the monopole part of the interaction with the extended nucleus. The corresponding scheme is shown in Fig. 11. According to perturbation theory, the expression for the "muonic isomer shift" is of the form

$$\Delta E_{is} = e \int V_\mu(r)\,\Delta\rho(r)\,d\tau, \tag{9}$$

where $V_\mu(r)$ is the potential produced by the muon in the $1s_{1/2}$ state. Thus, the quantity ΔE_{is} is connected with the difference between the nuclear charge distributions $\Delta\rho(r)$ in the ground and excited states. To determine the shift

$$\Delta E_{exp} = E_\mu - E \tag{10}$$

it is necessary to measure simultaneously with good accuracy the energy E_μ of the transition in the presence of the muon, and the corresponding energy in the usual radioactive source. If the magnetic splitting cannot be resolved in this case, then allowance must be made for corrections due to the magnetic hyperfine splitting, to the character of the population of the hyperfine-structure components at the initial instant, and to the M1 transition[3,45,97] between the doublet components. For the nuclear $2^+ \rightarrow 0^+$ transition, even if $E_{is} = 0$, a pseudoisomer shift will be observed, and can reach a value $\Delta E^{\mu}_{exp} = -(3/2)\Delta E_m$. The limiting case takes place if the time during which the transition between the doublet components takes place is short in comparison with the lifetime of the nuclear 2^+ level. In the isotopes ^{190,192}Os it was possible to resolve the hyperfine-structure components (see Fig. 9) and determine experimentally the values of the corrections. In the remaining nuclei, these corrections must be calculated. In the isotopes ^{203,205}Tl it was also possible to resolve the splitting of the ground state. For the $3/2^+$ excited state, however, it was necessary to use the theoretical values of the corrections. The nuclear models used for the calculation (the single-particle and the weak-coupling models) differ quite strongly, so that the correction has not been uniquely determined to date.

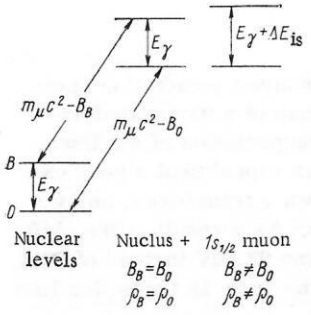

Fig. 11. Muonic isomer shift: E_γ is the energy of γ radiation; $E_0(E_B)$ is the binding energy of the $1s_{1/2}$ muon state calculated with allowance for the charge distribution $\rho_0(\rho_B)$ in the main excited state.

In the case of the $2^+ \rightarrow 0^+$ transition, the muonic isomer shift ΔE^{μ}_{is} is determined from the measured energy shift[92] with the aid of the relation

$$\Delta E^{\mu}_{is} = \Delta E_{exp} + \Delta E_m \left(\frac{3}{5} - \frac{2}{5} R_F\right) \Big/ (1 + R_F), \tag{11}$$

where

$$R_F = B_i \frac{T_{1/2}(M1)}{(1+B_i)\,T_{1/2}(I) + T_{1/2}(M1)}; \tag{12}$$

ΔE_m is the magnetic hyperfine splitting of the 2^+ level; B_i is the ratio of the populations of the states of the hyperfine structure with spins F = 5/2 and 3/2 at the initial instant, calculated with allowance for the resonant interaction; $T_{1/2}(I)$ is the half-life of the 2^+ state; $T_{1/2}(M1)$ is the half-life connected with the transition between the doublet components.

The results of all the measurements of the muonic isomer shift are listed[92] in Table 6. The theory of this phenomenon for deformed nuclei is developed in a splendid paper by Powers.[73]

Comparison of muonic and Mössbauer isomer shifts. In the investigation of the Mössbauer effect one measures a quantity that is essentially analogous to the muonic shift. The difference lies only in the fact that in the former case one determines the difference between the shifts due to different chemical compositions of the lattices:

$$\delta E = e \int [V_e^{(1)} - V_e^{(2)}]\,\Delta\rho(r)\,d\tau \approx \Delta\,|\psi(0)|^2\,\Delta\langle r^2\rangle + \text{small corrections}, \tag{13}$$

where $V_e^{(1)}$ and $V_e^{(2)}$ are the electronic potentials in two different chemical components. The quantity $\Delta|\psi(0)|^2$ is the difference between the electron densities. It must be calculated theoretically and is the cause of the principal uncertainty.[60] In the case of the muonic isomer shift, V_μ can be easily calculated by solving the Dirac equations. The presence of the electrons can then be completely neglected. It is expedient to "calibrate" $\Delta\cdot|\psi(0)|^2$ by comparing the results of the Mössbauer and muonic shifts. To this end it is necessary to satisfy the following conditions: It is necessary to have experimental data both on the muonic and on the Mössbauer shift; the isomer shift should be sufficiently large to make the accuracy of the results high; it is necessary to know the ratio of the muonic isomer shift ΔE^{μ}_{is} to the quantity $\Delta\langle r^2\rangle$. The density of the muonic function of the $1s_{1/2}$ level on the nuclear surface is only 30% of the central density, whereas the electron density is almost constant in the volume of the nucleus. The Mössbauer isomer shift is therefore sensitive only to changes in $\Delta\langle r^2\rangle$, whereas the muonic shift is determined by other moments of the charge distribution. For example, for heavy atoms the muonic shift determines a quantity close to $\Delta\langle r^{1,2}\rangle$. It follows therefore that there is no direct connection between the data of the two experiments, but a connection

TABLE 6. Excitation Probabilities P_μ and Isomer Shifts ΔE_{is} of Nuclear Levels of Different Muonic Atoms. The Errors Shown Take into Account Possible Uncertainties in the Calculations of the Corrections Necessitated by the Magnetic Hyperfine Splitting

Isotope	Level		P_μ, %/μ stoppings	ΔE_{is}, eV
	E_e, keV	I^π		
$^{150}Nd_{60}$	130.2	2+	—	900±130 *
$^{152}Sm_{62}$	121.8	2+	30±7	850±70
	121.8	2+	—	910±80 *
$^{154}Gd_{64}$	123.1	2+	—	1120±150 *
$^{156}Gd_{64}$	89.0	2+	33±8	5±100
$^{158}Gd_{64}$	79.5	2+	46±11	−235±70
$^{160}Gd_{64}$	75.3	2+	58±14	−80±180
$^{166}Er_{68}$	80.6	2+	—	10±160
$^{170}Yb_{70}$	84.3	2+	45±11	50±60
$^{182}W_{74}$	100.1	2+	41±10	0±110
	100.1	2+	—	−30±120 *
$^{184}W_{74}$	111.2	2+	44±10	0±80
	111.2	2+	—	10±120 *
$^{186}W_{74}$	122.6	2+	37±8	−40±70
	122.6	2+	—	10±120 *
$^{188}Os_{75}$	155.0	2+	51±14	−55±55
	633.1	2+	8±2	1380±150
	790.0	3+	6±2	
$^{190}Os_{76}$	186.7	2+	34±8	-145^{+65}_{-45}
	558.0	2+	5.4±1.5	1440±120
$^{192}Os_{76}$	205.8	2+	22±5	−195±60
	489.1	2+	3.3±0.7	760±100
	690.4	3+	0.8±0.2	650±200
$^{194}Pt_{78}$	328.5	2+	17±3	300^{+180}_{-60}
	622.1	2+	7.8±2.0	310^{+190}_{-90}
$^{196}Pt_{78}$	355.7	2+	12±3	390^{+330}_{-280}
$^{198}Hg_{80}$	411.8	2+	27±10	490^{+110}_{-270}
$^{200}Hg_{80}$	368.0	2+	12±4	-550^{+160}_{-200}
$^{202}Hg_{80}$	439.5		3.7±1.5	-15^{+190}_{-320}
$^{153}Eu_{63}$	83.4	7/2+	28.2±6.8	−65±130
	97.4	5/2−	0.7±0.8	−4845±160
	103.2	3/2+	4.2±1.6	−6036±150
	151.6	7/2−	3.3±0.7	−5325±180
	172.9	5/2+	1.9±0.7	
	193.1	9/2+	5.4±1.1	130±160
	269.7	7/2+	1.4±0.3	
$^{169}Tm_{69}$	8.4	3/2+		−455±130
	118.2	5/2+	24±6	−317±120
	138.9	7/2+	4.6±1.5	−460±160
$^{181}Ta_{73}$	136.3	9/2+	25±6	80^{+270}_{-140}
	482.0	5/2+		−3400±1100
$^{185}Re_{75}$	125.3	7/2+	31±7	15±125
$^{187}Re_{75}$	134.2	7/2+	30±7	5±125
$^{191}Ir_{77}$	129.4	5/2+	22±5	80±120
$^{193}Ir_{77}$	139.3	5/2+	22±5	−10±150
$^{199}Hg_{80}$	158.4	5/2−	18±4	264±150
	208.2	3/2−	13±4	410±120
$^{203}Tl_{81}$	279.2	3/2+	4.0±1.0	−310±110
	203.7	3/2+	6.5±3.5	−650±110
	619.4	5/2+		−500±300
	923.8	7/2+		−1900±600
$^{205}Tl_{81}$	1140.7	3/2+		−2100±500
	1340.4	3/2+		−1200±400
	2623.1	5/2−		7100±1000
	1608.5	13/2+	1.3±0.7	3720^{+600}_{-760}
	1608.5	13/2+		3480±590 **
	2564.5	9/2+	2.7±0,8	6180±430
$^{209}Bi_{83}$	2564.5	9/2+	3.1 **	5800±490 **
	2741.0	15/2+	4.2±0.5	6780±450
	2741.0	15/2−	3.7 **	6250±380 **

* A. Gal et al.[45] and the literature cited therein.
** W. Y. Lee et al.[68]

can be established with the aid of reliable theoretical calculations.

The maximum isomer shift is observed in measurements of the Mössbauer effect for the 97-and 103-keV levels of ^{153}Eu. Since neither level belongs to the ground-state rotational band, theory[24,47] predicts a low probability of their excitation in muon cascade transitions. However, the experimentally observed intensity is quite large and amounts[89] to about 2%. The measured γ-radiation spectrum is shown in Fig. 12. The use of a variegated experimental technique for the interpretation of six lines of nuclear γ radiation makes this experiment a good example of identification of unknown γ transitions, and we shall therefore describe it here. As a result of the shift, the energy of the γ_1 transition was 93 keV instead of 97.4. Superimposed on this line was the $4p \rightarrow 1s$ transition line

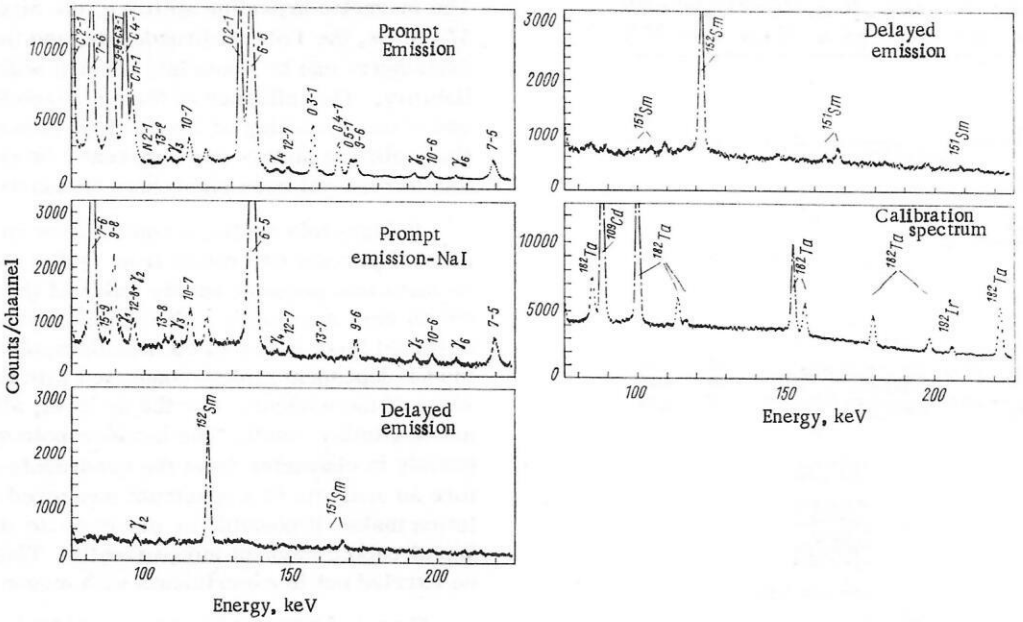

Fig. 12. Prompt, delayed, and calibration spectra[89] of muon activated Eu_2O_3 (natural isotope mixture). The background of the muonic atoms C, N, and O is noted: 1) delayed-emission spectrum measured with a delay from 15 to 35 nsec relative to the instant of muon stopping; 2) delayed-emission spectrum with delay from 35 to 300 nsec. The calibration was carried out by simultaneously measuring the emission from the source. The spectrum in the case of enriched ^{153}Eu is given in ref. 92.

in the carbon muonic atom, which was excluded by using a system of coincidences with the pulse in the NaI crystal (see below). The shift caused the energy of the γ_2 transition to be 97 keV instead of 103.2. The 12 → 8 transition line in the Eu muonic atom was superimposed on this line. However, the lifetime of the nuclear level was long and amounted to 5.4 nsec. The corresponding radiation was delayed relative to the prompt 12 → 8 transition, thus facilitating separation of the nuclear level. The background did not affect the remaining four γ lines, from γ_3 to γ_6. A line from the 7 → 6 transition in the muonic atom was superimposed on the strong 83.37-keV γ line corresponding to the transition to the first rotational state. No experimental trickery was capable of getting rid of the 7 → 6 line, whose intensity was large because of the anomalously high intensity of the 7 → 6 transition (see Fig. 5 of ref. 92). The identified γ transitions in the ^{153}Eu nucleus are shown on the level scheme (Fig. 13) together with the values of the muonic isomer shift. By taking into account the result of ref. 73 it is possible to obtain the electron density difference $\Delta|\psi(0)|^2 = (2.67 \pm 0.30) \cdot 10^{26}$ cm^{-3} between the divalent and trivalent states[92] of Eu.

This "calibration" of the Mössbauer isomer shift can be extrapolated also to other rare-earth nuclei[89] and yields more reliable information on $\Delta\langle r^2\rangle$. Comparing the values of $\Delta\langle r^2\rangle$ obtained in this manner with data on $\Delta\langle r^k\rangle$ by starting from the muonic isomer shift, we can determine the variation of the charge-distribution parameters c and t on going from the ground state to the excited state. An attempt at such an analysis was made in ref. 91, but the large ambiguities arising in the determination of various corrections have not made it possible to reach a definite conclusion.

4. QUADRUPOLE INTERACTION IN MUONIC ATOMS

Hyperfine quadrupole splitting of 2p → 1s and 3d → 2p lines. It was already noted above that owing to the presence of magnetic dipole (M1) and electric quadrupole (E2) interaction between the muon and the nucleus, the levels of the muonic atom become split. The quadrupole interaction is proportional to m_μ^3 and the magnetic-dipole interaction to m_μ^2. The quadrupole splitting in muonic atoms, unlike ordinary atoms, therefore exceeds the magnetic dipole splitting. In deformed nuclei with large quadrupole moments, the resultant splitting is comparable with the fine splitting and amounts[53,94,95,98] to 100-200 keV. In addition to the static quadrupole interaction there is also a strong dynamic E2 interaction that leads to resonant excitation of the rotational nuclear states. This effect has already been discussed. As a result of this interaction, a large quadrupole splitting will also be observed in strongly deformed nuclei with I = 0. By way of illustration we can cite Fig. 26 of ref. 99, devoted to a study of tungsten isotopes.

The static quadrupole interaction in muonic atoms is calculated in analogy with the ordinary atom.[30,99] However, owing to the strong mixing of the muonic and rotational nuclear states, it is necessary in the case of deformed nuclei to carry out detailed calculations of the influence of the off-diagonal matrix elements (see, e.g., ref. 98). Within the framework of definite nuclear models one can relate the internal and spectroscopic quadrupole moments, and also the deformation parameter β and the quantity $B(E2, 0^+ \rightarrow 2^+)$. Therefore only one parameter is free, and it is this parameter which must be determined from the experimental data. We emphasize that

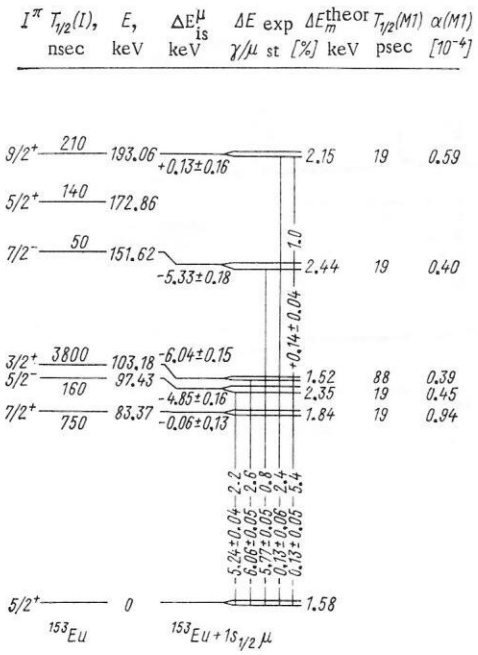

Fig. 13. Level scheme[92] of ^{153}Eu (left) and the level splitting (right) due to the presence of a muon on the $1s_{1/2}$ orbit: ΔE^{theor} – calculated value of the magnetic hyperfine splitting; $\alpha(M1)$ – conversion coeffcient for the transition between the doublet components; γ/μ_{st} – γ-emission intensity per muon stopping in ^{153}Eu.

the result of such a reduction of the experimental data depends strongly on the model assumptions. Moreover, allowance for the polarizability of the nucleus[75] also changes the value of the quadrupole splitting. First attempts at such an analysis did not lead to unambiguous conclusions concerning the nuclear models.[93] For future investigations it is essential to have a better resolution and a combined reduction of the experimental data with the use of exact values of the quadrupole moments obtained from transitions between high-lying states of the muonic atom. It must be recognized here that the internal quadrupole moments of the ground and excited states may differ.[63]

Model-independent precision measurements of quadrupole moments. In muonic atoms, the finite dimensions and the polarizability of the nucleus do not influence the binding energy and the quadrupole splitting of the high-lying levels (e.g., the $4f$ level), since the quadrupole moment can be determined from the splitting independently of the model. The splitting in this case is, however, much smaller than for the low-lying $2p_{3/2}$ level. It is therefore necessary to use Ge(Li) detectors with high resolution. The results of the first such measurements are shown in Fig. 14. A preliminary result of the reduction of the experimental data leads to a quadrupole moment $Q = 3.74 \pm 0.05$ b for the ^{157}Lu nucleus.[31] Although the effects of the finite dimensions and polarizability of the nucleus are small for the $4f$ level (the $3d$-level corrections for these effects amount to only 4%), it is necessary nevertheless to take into account a number of other corrections to make the accuracy of the final result not worse than 1%. In $5 \rightarrow 4$ transitions one can usually neglect the excitation of the nucleus. Caution is necessary, however, since a resonance can occur accidentally, as is the case[92] in the $7 \rightarrow 6$ transition of the ^{153}Eu muonic atom.

The magnetic hyperfine splitting, the mixing of the $4f$ and $5f$ levels, the Lorentz broadening, and the observed line asymmetry can be taken into account with sufficient reliability. The influence of the polarizability of vacuum and of the screening of the electron cloud on the hyperfine-splitting picture can apparently be neglected, although this has not yet been rigorously demonstrated anywhere.

In high-spin nuclei, a contribution on the order of several percent can result from taking the hexadecapole moment into account, but the value of this moment is not known very accurately. The main uncertainty in the case of the $3d$ level is due to the hexadecapole splitting and to model-dependent effects connected with the finite dimensions of the nucleus. For the $4f$ level, all these effects are negligibly small. The hexadecapole splitting differs greatly in character from the quadrupole splitting. Therefore an analysis of a spectrum measured with high resolution makes it possible in principle to determine the hexadecapole moment independently. This program can be carried out in experiments with meson factories.

Quadrupole effects related to strong interaction in pionic atoms. In pionic atoms produced from deformed nuclei with spins $1 > 1$, just as in muonic atoms, a hyperfine quadrupole level splitting with orbital angular momentum $l \geq 1$ is produced. There is, however, a certain difference between these two types of atoms. In pionic atoms the splitting can be observed only for high-lying levels that are not greatly affected by the strong interaction of the pions with the nucleons of the nucleus. For the low-lying levels, the intensity of the cascade transitions is small because of the strong pion-absorption effect.[9] The pion in the field of the nucleus is described by the Klein–Gordon equation and not by the Dirac equation, and the strong interaction with the nucleons must be taken into account, say with the aid of an optical potential.

The level shift in pionic atoms was calculated in ref. 80. According to that reference, the energy shift of the hyperfine component, due to the quadrupole interaction, is

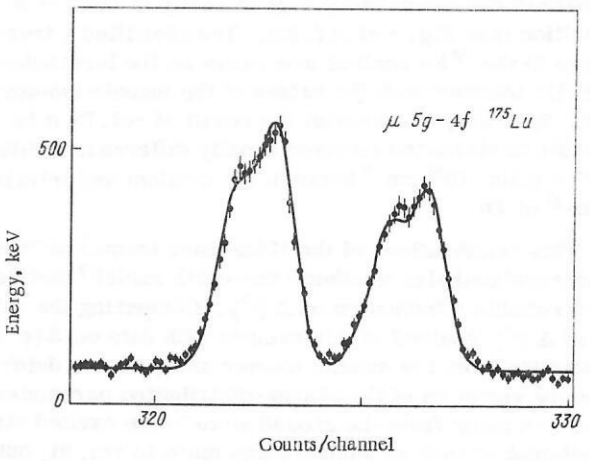

Fig. 14. Spectrum of $\mu 5g \rightarrow 4f$ transition in the ^{175}Lu muonic atom:[31] solid line – result of preliminary least-squares reduction. The quadrupole moment turned out to be 3.74 ± 0.05 b.

$$\Delta W(I,\ l,\ F) = A_2 C(I,\ l,\ F), \tag{14}$$

where

$$C(I,\ l,\ F) = \frac{3X(X-1) - 4I(I+1)\,l(l+1)}{2I(2I-1)\,l(2l-1)}; \tag{15}$$

$$X = I(I+1) + l(l+1) - F(F+1). \tag{16}$$

The quantities in the equations are so defined that C(I, l, F) = 1 when F assumes its maximum values $F_{max} = 1+l$. For estimates we can use the value of A_2 obtained in the point nucleus approximation and using nonrelativistic hydrogenlike wave functions:

$$A_2 \approx e^2 Q \left(\frac{Z}{a_\pi}\right)^3 \frac{1}{n^3 (l+1)(2l+1)(2l+3)}, \tag{17}$$

where $a_\pi = 194$ F.

The expressions for the shift due to the strong interaction and for the hyperfine-structure level width are

$$\varepsilon(F) = \varepsilon_0 + \varepsilon_2 C(I,\ l,\ F); \tag{18}$$

$$\Gamma(F) = \Gamma_0 + \Gamma_2 C(I,\ l,\ F), \tag{19}$$

where the quantities ε_0 and Γ_0 are connected with the monopole part of the strong-interaction potential. The additional shift ε_2 and the width Γ_2 are proportional to the energy of the static electric E2 interaction. As shown in ref. 80, the following approximate relation is valid:

$$\frac{\varepsilon_2}{\varepsilon_0} \approx \frac{\Gamma_2}{\Gamma_0} \approx \frac{5l}{8\pi(2l+3)} \cdot \frac{\int_0^\infty \rho_2(r)\, r^{2l+2}\, dr}{\int_0^\infty \rho_0(r)\, r^{2l+2}\, dr}. \tag{20}$$

As a result the expressions used to reduce the experimental spectrum acquire only one new parameter in addition to the unperturbed energy ε_0 and the unperturbed width Γ_0.

For the sake of clarity we can draw the following simple picture, which illustrates the effect of the quadrupole interaction: In the field of the deformed nucleus, each hyperfine-structure level with spin F has a definite spatial orientation relative to the deformation axis of the nucleus. The overlap of the wave function with the region of distribution of nuclear matter is therefore somewhat different for each state. Thus, the hyperfine-structure levels, being differently oriented relative to the deformation axis and reflecting primarily the mass distribution on the surface of the nucleus, depend on the moment $\langle r^{2l} \rangle$ obtained with the quadrupole deformed density component ρ_2. The picture of the hyperfine splitting of the $4f$ level of the ^{175}Lu pionic atom is given in Fig. 1 of ref. 80.

Since the quadrupole effect ε_2 due to the strong interaction is small (it amounts[80] to only 3.2% for the $4f$ level of the ^{175}Lu pionic atom), it follows that the normal static quadrupole moment should be known at least with the same accuracy. The ratio ε_2/A_2 is proportional to the difference between the exact value of the quadrupole moment, obtained from data on transitions between high-lying states, and the effective quadrupole moment determined from the $5 \rightarrow 4$ transition.

The first attempts at such investigations were reported in ref. 32. It follows from the preliminary analysis that the effective quadrupole moment is approximately 20% larger than the value obtained from transitions in muonic atoms. A final conclusion, however, calls for taking into account all the corrections referred to in Sec. 4.

5. FURTHER DEVELOPMENT OF THE EXPERIMENTAL TECHNIQUES FOR THE STUDY OF MUONIC ATOMS

The general scheme of the experiments in which muonic atoms are investigated has been described in many papers.[2,5,72,77,99] We shall therefore discuss here only certain questions connected with further development of the experimental techniques.

Background due to radiation from the light muonic atoms of carbon, nitrogen, and oxygen. The K and L series of light muonic atoms (of carbon, nitrogen, and oxygen) are observed as a background in all the measurements. These elements are contained in the materials of the apparatus itself (plastic scintillators, Plexiglas light pipes, etc.). The transition energies in such systems frequently coincide with the energy of the x-ray or nuclear γ radiation of the heavy muonic atom. The use of scintillators and light pipes that contain no oxygen atoms and the use of gaseous helium in the anticoincidence counters decrease the intensities of the lines corresponding to nitrogen and oxygen without affecting the carbon lines. By using an additional coincidence circuit, it is possible to suppress these lines almost completely.[24,47,92] If a large (5" × 4") NaI crystal is placed in line with the target, it will detect γ quanta of energy higher than 50-80 keV. A germanium detector operating in coincidence with the crystal selects only events pertaining to heavy muonic atoms, and does not detect events from light atoms. In particular, in the case of oxygen the crystal transmits only the line corresponding to the $2p \rightarrow 1s$ transition, since the energy is equal to 134 keV, which exceeds the detection threshold. As to the L series, the energy of such transitions is only 25-45 keV. The setup will not record any cascade in coincidence with the $2p \rightarrow 1s$ line of oxygen. For heavy muonic atoms, the energies of the transitions from the orbits up to n = 8 exceed the threshold energy and the apparatus will record the entire cascade. The intensity of the x rays from heavy muonic atoms is attenuated thereby to 20-50%, depending on the dimensions and geometry of the crystal and on the charge Z of the target, while that of the light muonic atoms will be attenuated by a factor larger than 100. By way of illustration, Fig. 12 shows the spectrum of the muonic atom of Er measured using the procedure discussed above. Another example is Fig. 2 of ref. 39.

Energy calibration. Energy calibration is one of the principal problems in experiments with muonic atoms. When comparing the x-ray emission of a muonic atom with the γ emission of a radioactive source, account must be taken of effects that influence the line position. The temporal distribution of the x-ray emission intensity is a reflection of the temporal structure of the

accelerator pulse, whereas the intensity of the calibration γ line is constant in time. The line position depends on the counting rate of the Ge(Li) detector and varies in time because of the usual instability of the entire system, consisting of the preamplifier and the analog–digital converter. The calibration signal must therefore be detected under the same temporal conditions as the events themselves. This can be done by detecting the calibration symbol with the aid of random coincidences to the counter signals, whose intensity is proportional to the muon-beam intensity.[5] In addition to the difference in the temporal structure, the target and radioactive source differ in dimensions and in their placements relative to the Ge(Li) detector. The appropriate correction must be taken into account.

All the foregoing difficulties can be avoided if the calibration line is emitted as a result of interaction of the muon beam with the target itself. The only process that can be used for this purpose involves the muon-absorption reaction, for example

$$^{203}\mathrm{Tl}\,(\mu^-,\ \nu n)\,^{202}\mathrm{Hg}^* \rightarrow {}^{202}\mathrm{Hg} + \gamma\,(439.54\,\mathrm{keV}). \qquad (21)$$

The same γ emission can simultaneously be obtained from a radioactive ^{202}Tl source. Comparison of the two lines in one experiment will provide a check on the reliability and accuracy of the calibration procedure. The attained accuracy is 20 eV at energies[90] up to 500 keV.

[1)] The calculations were carried out with the wave function of the muon in the field of an extended nucleus.

[2)] The magnetic moments turned out to be $\mu(^{190}\mathrm{Os}) = 0.694$ and $\mu(^{192}\mathrm{Os}) = 0.756$. The experimental values are given in Table 5.

[1] H. L. Acker et al., Nucl. Phys., 87, I (1966).
[2] H. L. Anderson et al., Phys. Rev., 187, 1565 (1969).
[3] R. Baader et al., Phys. Lett., B27, 425 (1968).
[4] H. Backe, Z. Phys., 241, 435 (1971).
[5] H. Backe et al., Nucl. Phys., A189, 472 (1972).
[6] H. Backe et al., Verh. der deutsch. Phys. Gesellschaft, 1, E5.1, p. 112.
[7] G. Backenstoss et al., Phys. Lett., B25, 547 (1967).
[8] G. Backenstoss et al., Phys. Lett., B31, 233 (1970).
[9] G. Backenstoss, Ann. Rev. Nucl. Sci., 20, 467 (1970).
[10] G. Backenstoss, Fourth Int. Conf. on High-Energy Physics and Nuclear Structure, Dubna (1971), p. 283.
[11] G. Backenstoss et al., Phys. Lett., 41, 522 (1972).
[12] G. Backenstoss et al., Phys. Lett., B43, 539 (1973).
[13] S. Barshay, Phys. Lett., B37, 397 (1971).
[14] S. Barshay, Phys. Rev., 7, 2635 (1973).
[15] T. L. Bell, Phys. Rev., A7, 1480 (1973).
[16] H. A. Bentz, Z. Phys., 243, 138 (1971).
[17] I. Ben-Zvi et al., Nucl. Phys., A151, 401 (1970).
[18] J. Blomqvist, Nucl. Phys., B48, 95 (1972).
[19] A. Bohr and V. F. Weisskopf, Phys. Rev., 77, 94 (1950).
[20] E. Campani, Nuovo Cimento Lett., 4, 982 (1970).
[21] R. A. Carrigan et al., Phys. Rev. Lett., 20, 874 (1968).
[22] R. A. Carrigan et al., Bull. Amer. Phys. Soc., 13, 65 (1968).
[23] M. Y. Chen, Nucl. Phys., A181, 25 (1972).
[24] Y. K. Chen and W. Pieper, Z. Phys., 220, 185 (1969).
[25] S. C. Cheng et al., Phys. Lett., B34, 615 (1971).
[26] S. Cohen, Report UCRL-8389 (1958).
[27] R. K. Cole, Jr., Phys. Rev., 177, 164 (1969).
[28] H. Crannel, Phys. Rev., 148, 1107 (1966).
[29] E. B. Dally et al., Phys. Rev., C2, 2057 (1970).
[30] S. Devons and I. Duerdoth, Adv. Nucl. Phys., 2, 295 (1969).
[31] W. Dey et al., Proc. Intern. Conf. on Nuclear Moments and Nuclear Structure, Osaka, 1972 (Osaka, Japan), p. 261.
[32] W. Dey et al., Proc. Intern. Conf. on Nuclear Moments and Nuclear Structure, Osaka, 1972 (Osaka, Japan), p. 263.
[33] M. S. Dixit et al., Phys. Rev. Lett., 27, 878 (1971).
[34] T. Dubler et al. (in press).
[35] J. Eisinger and V. Jaccarino, Rev. Mod. Phys., 30, 528 (1958).
[36] R. Engfer, Proc. Intern. School Physics "Enrico Fermi," Course 38, Interaction of High-Energy Particles with Nuclei, T. E. O. Ericson (ed.), Academic Press, New York (1967), p. 64.
[37] R. Engfer and D. Türk, Z. Phys., 205, 90 (1967).
[38] R. Engfer and F. Scheck, Z. Phys., 216, 274 (1968).
[39] R. Engfer, Proc. Third Intern. Conf. on High-Energy Physics and Nuclear Structure, Columbia Univ., 1969, S. Devons (ed.), Plenum, New York (1970), p. 104.
[40] T. E. O. Ericson and J. Hüfner, Phys. Lett., B40, 459 (1972).
[41] T. E. O. Ericson and J. Hüfner, Nucl. Phys., B47, 205 (1972).
[42] B. Fricke, Nuovo Cimento Lett., 2, 859 (1969).
[43] B. Fricke, Z. Phys., 218, 495 (1969).
[44] B. Fricke, J. T. Waber, and V. L. Telegdi, Preprint COO-212734, 1972 (in press).
[45] A. Gal, L. Crodzins, and J. Hüfner, Phys. Rev. Lett., 21, 453 (1968).
[46] A. Di Giacomo, Nucl. Phys., B11, 411 (1969).
[47] K. Göke and H. Marschall, Z. Phys., 218, 308 (1968).
[48] E. K. Henley and L. Wilets, Phys. Rev. Lett., 20, 1389 (1968).
[49] J. Hüfner, Z. Phys., 190, 81 (1966).
[50] J. Hüfner, Phys. Lett., B25, 189 (1967).
[51] J. Hüfner and F. Scheck, in: Muon Physics, V. W. Hughes and C. S. Wu (eds.), Academic Press, New York (1973).
[52] G. Islam, J. Meyer, and J. Speth, (in press); Proc. Intern. Conf. on Nucl. Nucl. Phys., 1, 309 (1973).
[53] B. A. Jacobsohn, Phys. Rev., 96, 1637 (1957).
[54] J. A. Jansen, Thesis IKO, Amsterdam (1971).
[55] J. A. Jansen, R. Th. Peerdeman, and C. de Vries, Nucl. Phys., A188, 337 (1972).
[56] D. A. Jenkins et al., Phys. Lett., B32, 267 (1970).
[57] D. A. Jenkins et al., Nucl. Phys., 175, 73 (1971).
[58] J. A. Johnson et al., Phys. Lett., B29, 420 (1969).
[59] J. Johnson and R. A. Sorensen, Phys. Rev., 2, 102 (1970).
[60] G. M. Kalvius, Hyperfine Interaction in Excited Nuclei, Vol. 3, G. Goldring and R. Kalish (eds.), Gordon and Breach, New York (1971), p. 523.
[61] Y. N. Kim, Mesic Atoms and Nuclear Structure, North-Holland, Amsterdam (1971).
[62] W. C. King et al., Phys. Rev., C4, 1382 (1971).
[63] T. Konishi, Progr. Theor. Phys., 48, 1569 (1972).
[64] B. E. Lautrup, A. Peterman, and E. de Rafael, Phys. Reports, C3, 192 (1972).
[65] M. Le Bellac, Nucl. Phys., 40, 645 (1963).
[66] W. Y. Lee et al., Phys. Rev. Lett., 23, 648 (1969).
[67] W. Y. Lee et al., Nucl. Phys., A167, 652 (1971).
[68] W. Y. Lee et al., Nucl. Phys., A181, 14 (1972).
[69] R. Link et al., Phys. Lett., B37, 50 (1971).
[70] R. Link et al., Phys. Lett., B42, 57 (1972).
[71] R. Link, Doktorarbeit Inst. f. Techn. Kernphys. Technische Hochschule, Darmstadt.
[72] R. J. McKee et al., Nucl. Instrum. Methods, 92, 421 (1971).
[73] J. Meyer and J. Speth, Phys. Rev. A (in press); J. Meyer and J. Speth, Dubna preprint E4-4873; Yad. Fiz., 17, 1197 (1973) [Sov. J. Nucl. Phys., 17, 623 (1973)]; J. Meyer, P. Ring, and J. Speth (in press).
[74] Chen Min-Yi, Phys. Rev., C1, 1167 (1970).
[75] Chen Min-Yi, Phys. Rev., C1, 1176 (1970).
[76] H. P. Povel, Thesis, Kernforschungszentrum Karlsruhe, KFK 1602 (1972); H. P. Povel, Nucl. Phys., A (in press).
[77] R. G. Powers, Phys. Rev., 169, 1 (1968).
[78] G. A. Rinker and L. Wilets, Report LA-DC-72-1515 (1972).
[79] A. de Schalit, Phys. Rev., 122, 1530 (1961).
[80] F. Scheck, Nucl. Phys., B42, 573 (1972).
[81] W. Schütz, private communication; W. Schütz, Verh. d. deutschen physik Gessellschaft, 1, 149 (1973).
[82] H. F. Skardhamar, Nucl. Phys., A151, 154 (1970).
[83] I. Sick et al., Nucl. Phys., A150, 631 (1970).
[84] H. H. Stroke, R. J. Blin-Stoyle, and V. Jaccarino, Phys. Rev., 123, 1326 (1961).
[85] M. K. Sundaresan and V. Srinivasan, Phys. Rev. Lett., 21, 1509 (1968).

[86]M. K. Sundaresan and P. J. S. Watson, Phys. Rev. Lett., 29, 15 (1972).
[87]H. Theissen, Habilitationsschrift, T. H. Darmstadt (1972).
[88]P. Vogel, Report CALT-63-188 (1973).
[89]H. K. Walter et al., Phys. Lett., B33, 64 (1972).
[90]H. K. Walter et al., Phys. Lett., B40, 197 (1972).
[91]H. K. Walter et al., Helv. Phys. Acta, 45, 47 (1972).
[92]H. K. Walter et al. (in press).
[93]A. O. Vaisenberg, The Muon [in Russian], Nauka, Moscow (1964).
[94]J. A. Wheeler, Phys. Rev., 92, 812 (1953).
[95]L. Wilets and K. Danske, Vidensk. Selsk. Mat.-Fys. Medd., 29, No. 3 (1954).
[96]R. Wilson et al., Ann. Rev. Nucl. Sci., 14, 135 (1964).
[97]R. Winston, Phys. Rev., 129, 2766 (1963).
[98]R. A. de Wit et al., Nucl. Phys., 87, 657 (1967).
[99]C. S. Wu and L. Wilets, Ann. Rev. Nucl. Sci., 19, 527 (1969).
[100]C. S. Wu, Proc. Fourth Intern. Conf. on High-Energy Physics and Nuclear Structure, Dubna (1971), p. 349.
[101]D. F. Zaretskii and V. M. Novikov, Zh. Eksp. Teor. Fiz., 42, 511 (1962) [Sov. Phys.-JETP, 15, 358 (1962)].
[102]E. Zavattini, Proc. of the Topical Meeting on Intermediate Energy Physics, Zuoz (1973), organized by SIN-CERN; E. Zavattini, private communication.